

MATHEMATICAL AND NUMERICAL CHALLENGES IN DIFFUSE OPTICAL TOMOGRAPHY (DOT) FOR BREAST SCREENING

P. Causin (in collaboration with G. Naldi, M.Lupieri, R.Weishaeupl)

University of Milano



Scope of the work:

- Accurate numerical solutions
 - Short computational times
- } → cornerstones for marketable DOT devices

Scope of the work:

- Accurate numerical solutions
 - Short computational times
- } → cornerstones for marketable DOT devices

DOT employs **near-infrared** (NIR, 600 – 900 *nm*) light to illuminate the biological tissue *in vivo*.

DOT Inverse problem: Infer the optical parameter (biomarkers of pathogenic processes) “inverting” a mathematical model for light propagation in tissue based on experimental measurements of the light fluence.

Scope of the work:

- Accurate numerical solutions
 - Short computational times
- } → cornerstones for marketable DOT devices

DOT employs **near-infrared** (NIR, 600 – 900 *nm*) light to illuminate the biological tissue *in vivo*.

DOT Inverse problem: Infer the optical parameter (biomarkers of pathogenic processes) “inverting” a mathematical model for light propagation in tissue based on experimental measurements of the light fluence.

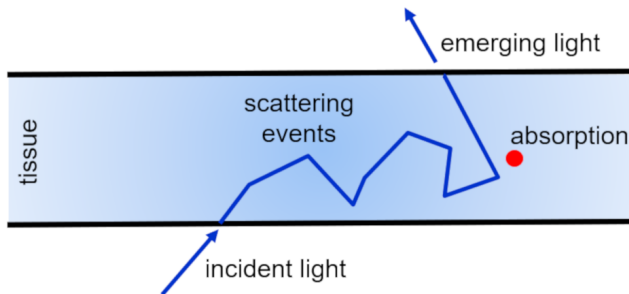
- Non-invasive
- Non-ionizing radiation

Optical Properties of Biological Tissue

The propagation of light through biological tissues is affected by **absorption** and **scattering** characterized by the absorption coefficient (μ_a [cm^{-1}]) and the scattering coefficient (μ_s [cm^{-1}]), respectively.

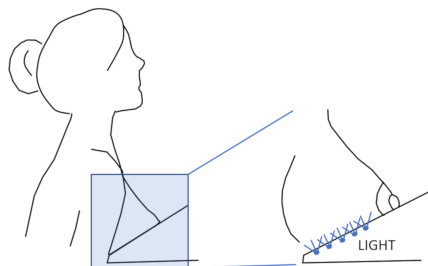
Optical Properties of Biological Tissue

The propagation of light through biological tissues is affected by **absorption** and **scattering** characterized by the absorption coefficient (μ_a [cm^{-1}]) and the scattering coefficient (μ_s [cm^{-1}]), respectively.



In the NIR spectral window the scattering effect can be **100x** larger than absorption. Due to the strong scattering light photons travel in tortuous paths.

We address the application of DOT to female **breast screening** to detect possible **cancerous lesions**.



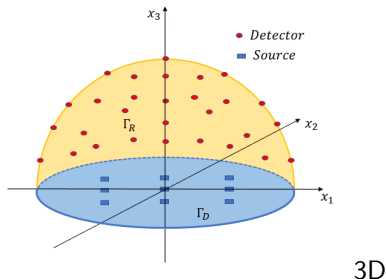
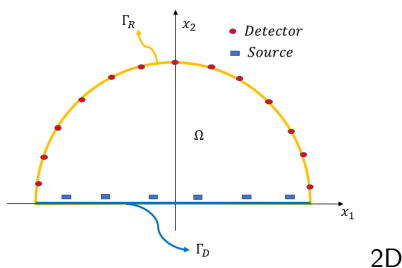
We address the application of DOT to female **breast screening** to detect possible **cancerous lesions**.

- **Geometry and source-detector arrangement**

Female breast supported on a solid plate.

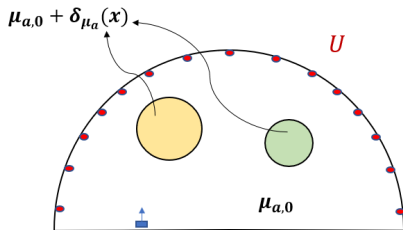
Γ_D : tissue-plate interface \rightarrow light sources,

Γ_R : tissue-air interface \rightarrow detectors.



Methodology

We address the application of DOT to female **breast screening** to detect possible **cancerous lesions**.



- **Light source**

LED modeled as Dirac delta source terms $S(x) = \delta(x - x_s)$, x_s source position.

- **Data**

For each source, light fluence U at the detectors.

- **Optical parameter to infer**

Absorption coefficient $\mu_a(x) = \mu_{a,0} + \delta\mu_a(x)$ (constant scattering coefficient).

Model for light propagation in tissue

Radiative transport equation (RTE) for the **light radiance**

\Downarrow if $\mu_s \gg \mu_a$
 P_1 approximation + stationary case

Diffusion Equation (DE)

$$-D\Delta U(x) + \mu_a(x)U(x) = S(x)$$

where $U(x)$ is the **photon fluence rate**, D is the **diffusion coefficient**.

Model for light propagation in tissue

Radiative transport equation (RTE) for the **light radiance**

\Downarrow if $\mu_s \gg \mu_a$
 \Downarrow P_1 approximation + stationary case

Diffusion Equation (DE)

$$-D\Delta U(x) + \mu_a(x)U(x) = S(x)$$

where $U(x)$ is the **photon fluence rate**, D is the **diffusion coefficient**.

Boundary Conditions for the fluence rate

Γ_D	tissue-plate interface	totally opaque plate	$U = 0$	Dirichlet BC
Γ_R	tissue-air interface	Fresnel reflection	$\frac{\partial U}{\partial \hat{n}} + \frac{1}{2AD}U = 0$	Robin BC

Rytov Approximation

Rytov approximation: $U(x) = e^{\psi(x)}$ where $\psi(x) = \sum_{i=0}^N \psi_i(x)$.

Rytov Approximation

Rytov approximation: $U(x) = e^{\psi(x)}$ where $\psi(x) = \sum_{i=0}^N \psi_i(x)$.

From the DE, under the 1st order Rytov approximation, defining the **Modified Helmholtz operator** $\mathcal{L} = \Delta - \frac{\mu_{a,0}}{D} \Rightarrow$

Problem for $U_0 = e^{\psi_0}$ *background fluence*

$$\begin{cases} \mathcal{L}U_0(x) = -\frac{1}{D}\delta(x - x_s) & x \in \Omega \\ U_0(x) = 0 & x \in \Gamma_D \\ \frac{\partial U_0}{\partial \hat{n}}(x) + \frac{1}{2AD}U_0(x) = 0 & x \in \Gamma_R \end{cases}$$

Problem for $U_0\psi_1$, $\psi_1(x) = \log \frac{U(x)}{U_0(x)}$ *logarithmic amplitude fluctuation of the light fluence*

$$\begin{cases} \mathcal{L}(U_0\psi_1)(x) = U_0(x)\frac{\delta\mu_a(x)}{D} & x \in \Omega \\ (U_0\psi_1)(x) = 0 & x \in \Gamma_D \\ \frac{\partial(U_0\psi_1)}{\partial \hat{n}}(x) + \frac{1}{2AD}(U_0\psi_1)(x) = 0 & x \in \Gamma_R \end{cases}$$

Green's Function method

$$\left\{ \begin{array}{ll} \mathcal{L}G(x, x') = \delta(x - x') & x \in \Omega \\ G(x, x') = 0 & x \in \Gamma_D \end{array} \right\} \rightarrow \text{Green Dipole } (G_D)$$
$$\left\{ \begin{array}{ll} \frac{\partial G}{\partial \hat{n}}(x, x') + \frac{1}{2AD} G(x, x') = 0 & x \in \Gamma_R \end{array} \right\} \rightarrow \text{Numerical approach}$$

Green's Function method

$$\left\{ \begin{array}{ll} \mathcal{L}G(x, x') = \delta(x - x') & x \in \Omega \\ G(x, x') = 0 & x \in \Gamma_D \end{array} \right\} \rightarrow \text{Green Dipole } (G_D)$$
$$\left\{ \begin{array}{l} \frac{\partial G}{\partial \hat{n}}(x, x') + \frac{1}{2AD} G(x, x') = 0 \\ x \in \Gamma_R \end{array} \right\} \rightarrow \text{Numerical approach}$$

Problem for $U_0\psi_1 \Rightarrow$

Linearized problem:

Fredholm integral equation of the first kind for $\delta\mu_a$

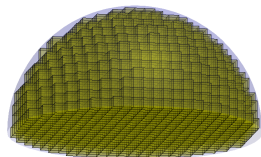
$$(U_0\psi_1)(x) = \int_{\Omega} G(x, x') \frac{\delta\mu_a(x')}{D} U_0(x') dx'$$

Discrete Inverse Problem 1/2

Starting from the Fredholm integral equation of the first kind

(1.) **evaluation** at the detector positions, $x = x_{d,\nu}$ for $\nu = 1, \dots, N_{Det}$ for each source position $x_{s,l}$ for $l = 1, \dots, N_{Src}$,

(2.) domain discretization through a **voxel-based mesh** composed of N_v elements of centroids $\{x_j\}_{j=1}^{N_v}$ and volumes $\{\Delta V_j\}_{j=1}^{N_v}$,



(3.) **midpoint quadrature rule** to discretize the integral,

(4.) use of the **dataset of measurements**:

$U^m(x_{d\nu}, x_{sl})$ and $U_0^m(x_{d\nu}, x_{sl})$ for $l = 1, \dots, N_{Src}$ and $\nu = 1, \dots, N_{Det}$.

Discrete Inverse Problem 2/2

From steps (1.) – (4.)

$$\log \left(\frac{U^m(x_{d,v}, x_{s,l})}{U_0^m(x_{d,v}, x_{s,l})} \right) \approx \sum_{j=1}^{N_v} \delta_{\mu_a}(x_j) \frac{\Delta V_j}{D U_0(x_{d,v}, x_{s,l})} \underbrace{U_0(x_j, x_{s,l}) G(x_{d,v}, x_j)}_{J_{i,j}}$$

$i \rightarrow \{l, v\}$

- Calculate
- Known from measurements or simulate

$$i = 1, \dots, M$$

$$M = N_{Src} \times N_{Det}$$

$$J \delta_{\mu_a} \approx y \quad \text{where } J \text{ is called } \mathbf{sensitivity\ matrix}$$

Discrete Inverse Problem

$$\delta_{\mu_a}^{LS} = \arg \min_x \mathcal{F}(x), \quad \text{where } \mathcal{F}(x) = \|Jx - y\|_2^2$$

Method of Fundamental Solutions

Goal: Find a numerical method to enforce the Robin BC that preserves high speed

Method of fundamental solutions (MFS) vs Boundary element method (BEM)

→ **MFS** is faster and provides more accurate results

Method of Fundamental Solutions

Goal: Find a numerical method to enforce the Robin BC that preserves high speed

Method of fundamental solutions (MFS) vs Boundary element method (BEM)

→ **MFS** is faster and provides more accurate results

Method of Fundamental Solutions

Goal: Find a numerical method to enforce the Robin BC that preserves high speed

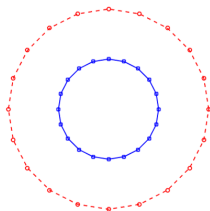
Method of fundamental solutions (MFS) vs Boundary element method (BEM)

→ **MFS** is faster and provides more accurate results

Single-layer potential representation on an auxiliary boundary Ω_a s.t. $\bar{\Omega} \subset \Omega_a$

$$u(x) = \int_{\partial\Omega_a} \sigma(\xi) G(x, \xi) dS_\xi$$

$$\text{Discretization} \Rightarrow u_{MFS}(x) = \sum_{j=1}^N a_j G(x, \xi_j)$$



▷ **Singularities:** $\{\xi_j\}_{j=1}^N \in \partial\Omega_a$

▷ **Collocation nodes:** $\{x_i\}_{i=1}^M \in \partial\Omega$

▷ **Unknowns:** $\{a_j\}_{j=1}^N$, determined imposing the BCs at the collocation nodes

$M \geq N \Rightarrow M \times N$ linear system for the unknowns a_j .

MFS convergence

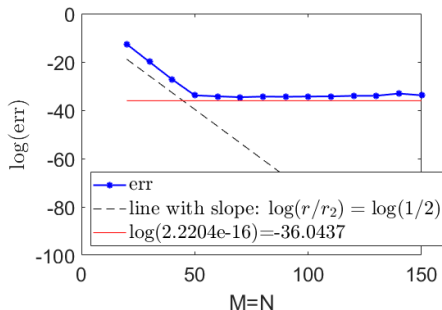
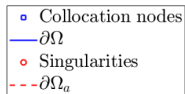
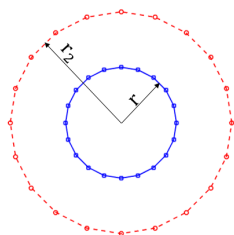
$$\|u - u_{MFS}\|_{L^2(\Omega)} = O\left(\left(\frac{r}{r_2}\right)^M\right)$$

$M = \# \text{collocation nodes}$

$N = \# \text{singularities}$

Test case in two-dimensions $[\Delta - k^2] u(x) = 0$ with $k = \sqrt{2}$.

Exact solution: $u(x) = e^{x_1 + x_2}$



MFS convergence

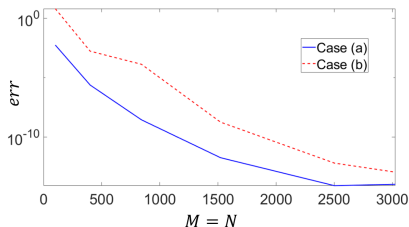
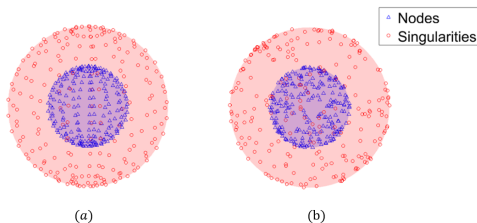
$$\|u - u_{MFS}\|_{L^2(\Omega)} = O\left(\left(\frac{r}{r_2}\right)^M\right)$$

$M = \# \text{collocation nodes}$

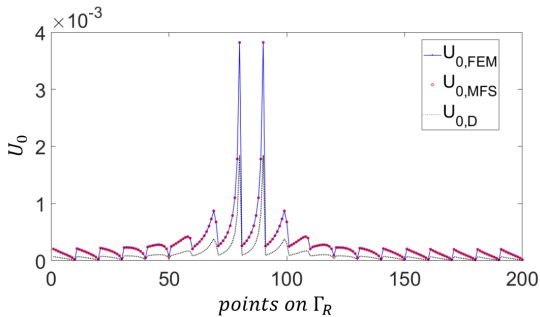
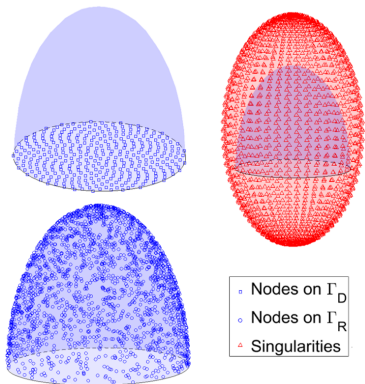
$N = \# \text{singularities}$

Test case in three-dimensions $[\Delta - k^2] u(x) = 0$ with $k = \sqrt{3}$.

Exact solution: $u(x) = e^{x_1 + x_2 + x_3}$

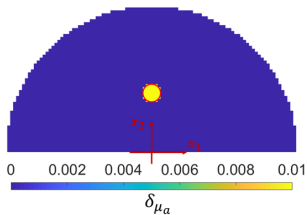


MFS for DOT

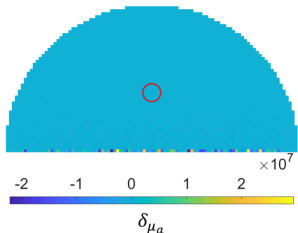
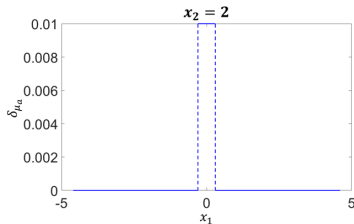


Necessity of Regularization

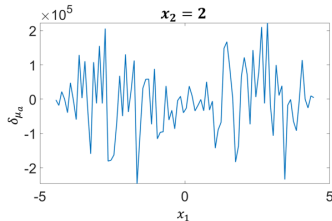
$$\delta_{\mu_a}^{LS} = \arg \min_{x \in \mathbb{R}^{N_v}} \mathcal{F}(x), \text{ where } \mathcal{F}(x) = \|Jx - y\|_2^2$$



Exact



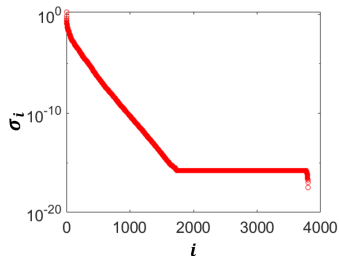
LS



Necessity of Regularization

$$\delta_{\mu_a}^{LS} = \arg \min_{x \in \mathbb{R}^{N_v}} \mathcal{F}(x), \text{ where } \mathcal{F}(x) = \|Jx - y\|_2^2$$

Singular values of the sensitivity matrix



Necessity of Regularization

$$\delta_{\mu_a}^{LS} = \arg \min_{x \in \mathbb{R}^{N_v}} \mathcal{F}(x), \text{ where } \mathcal{F}(x) = \|Jx - y\|_2^2$$

Regularization

$$\min_x \mathcal{F}(x) \text{ s.t. } \|x\|_p^p \leq \delta \Leftrightarrow \min_x \mathcal{F}_{\lambda,p}(x), \text{ where } \mathcal{F}_{\lambda,p}(x) = \mathcal{F}(x) + \lambda \|x\|_p^p$$

Necessity of Regularization

$$\delta_{\mu_a}^{LS} = \arg \min_{x \in \mathbb{R}^{N_v}} \mathcal{F}(x), \text{ where } \mathcal{F}(x) = \|Jx - y\|_2^2$$

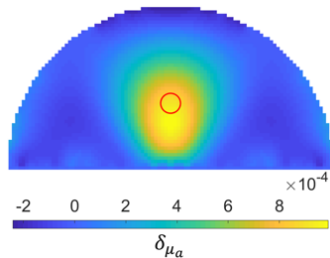
Regularization

$$\min_x \mathcal{F}(x) \text{ s.t. } \|x\|_p^p \leq \delta \Leftrightarrow \min_x \mathcal{F}_{\lambda,p}(x), \text{ where } \mathcal{F}_{\lambda,p}(x) = \mathcal{F}(x) + \lambda \|x\|_p^p$$

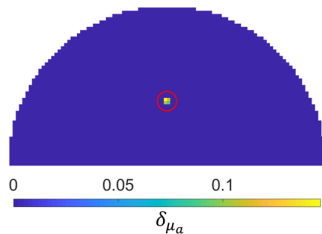
- **Tikhonov:** $p = 2$
- **LASSO:** $p = 1$

Regularization for DOT

Tikhonov



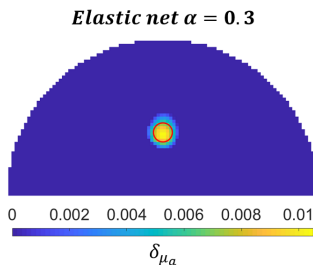
LASSO



	DOFS	$\ \delta\mu_a\ _\infty$
Exact	32	0.01
Tikhonov	$N_v = 3822$	$8 \cdot 10^{-4}$
LASSO	4	0.15

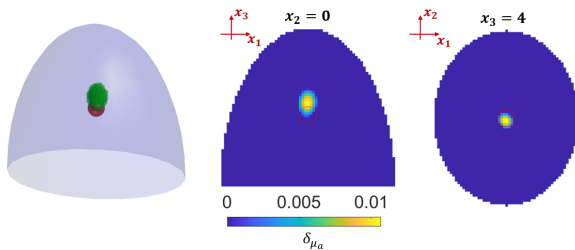
Regularization for DOT

Elastic net: $\min_x \mathcal{F}_{\lambda, \alpha}(x)$, where $\mathcal{F}_{\lambda, \alpha}(x) = \mathcal{F}(x) + \lambda\{\alpha\|x\|_1 + (1 - \alpha)\|x\|_2^2\}$,
 $\alpha \in [0, 1]$

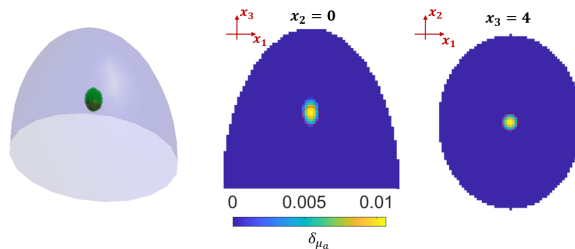


α	DOFS	$\ \delta_{\mu_a}\ _{\infty}$
Exact	32	0.01
0	N_v	$8 \cdot 10^{-4}$
0.1	178	$5 \cdot 10^{-3}$
0.2	119	$8 \cdot 10^{-3}$
0.3	93	0.01
0.4	74	0.013
0.5	63	0.016
0.6	51	0.02
0.7	37	0.025
0.8	24	0.03
0.9	17	0.06
1	4	0.15

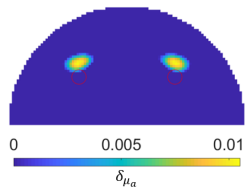
Dipole Approximation



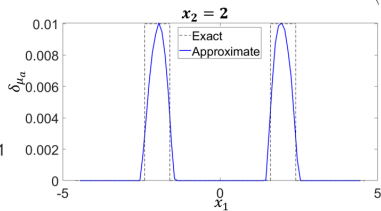
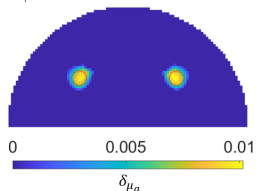
Robin BC (MFS)

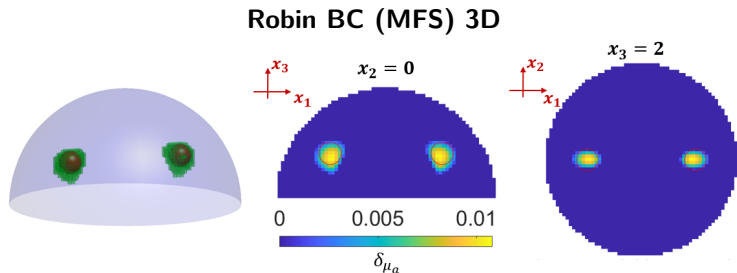


Dipole Approximation



Robin BC (MFS)

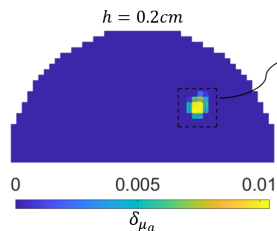




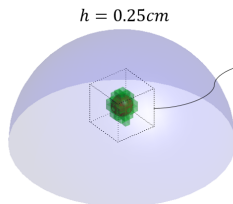
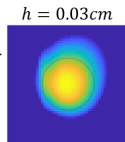
Computational Time in 3D		
$N_v = 72407$	Dipole Approximation	113 s
	Robin BC	160 s

Computational Time

Computational Time in 3D		
$N_v = 72407$	Dipole Approximation	113 s
	Robin BC	160 s



2D

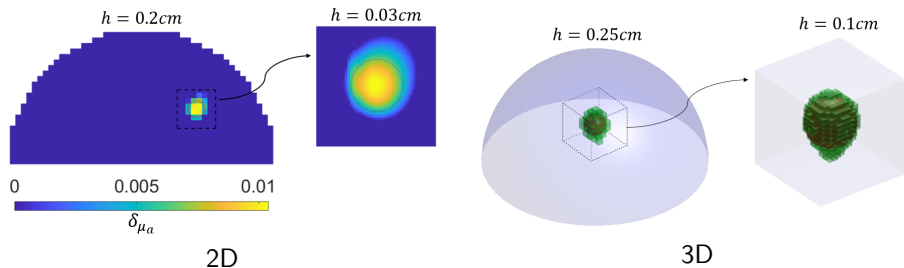


3D



Computational Time

Computational Time in 3D		
$N_v = 72407$	Dipole Approximation	113 s
	Robin BC	160 s



3D	N_v	Computational Time
$h = 0.1 \text{ cm}$ (whole domain)	72407	160 s
$h = 0.25 \text{ cm}$ (whole domain)	14876	30 s
$h = 0.1 \text{ cm}$ (cube of size 2 cm)	8000	17 s

} < 1min

Conclusions

The approach proposed accurately detects the inclusion/inclusions

- Size and intensity → **elastic net**
- Location → **enforcement of the Robin BC.**

The times of execution are short thanks to

- the choice of the framework: linearization under Rytov approximation adopting the DE as model equation
- the fast numerical method **MFS**
- a general **optimization**, in terms of computational costs, of the code.